Content and Context in Temporal Thalamocortical Binding

R. Llinás, U. Ribary, M. Joliot, and X.-J. Wang

Given that sensory systems generate but a fractured representation of universals, the issue of perceptual unity has been approached by defining the mechanisms by which different sensory components are gathered into one global image. In recent years, this has been described as "binding," and has been thought to be implemented by temporal conjunction (Bienenstock and von der Malsburg 1986, von der Malsburg 1981; Crick and Koch 1990; Llinás 1990).

Because the number of possible categories of perceptions is so extensive, their implementation via purely hierarchical connectivity is unlikely. Indeed, even considering that neuronal elements transduce signals and conduct information on the order of milliseconds beginning with the sensory primitives, to exhaust all the possibilities for sequential combinations would require some time. Even if each categorical perception were represented in its ultimate instance by the activity of a single cell, the number of categories may still be many orders of magnitude larger than the total number of possible "grandmother cells." This assumption is simplistic and it does not answer the question of how such cells may communicate their unique features to the rest of the nervous system, the nature of the messages from such cells, or the neurological deficits that their damage would produce. However, since categorizations are generated by spatial mapping of the primary sensory cortex and its associated cortical structures, perhaps a more dynamic interaction based on time parameters supplements such spatial maps. Thus, a secondary temporal mapping may be envisioned so as to accommodate the important role of simultaneity in the organization of perception.

The hypotheses to be discussed below are derived from two areas of research; first, from the investigation of single neuronal elements studied *in vitro* and *in vivo*; and second, from measurements made via noninvasive magnetoencephalography in humans. The main principal findings is that the intrinsic electrical properties of neurons and the dynamical events resulting from their connectivity produce global resonant states.

The Brain as a Closed System

Several lines of research suggest that the brain is essentially a closed system (Llinás 1988) capable of self-generated activity based on the intrinsic electrical properties of its component neurons and their connectivity. In such a view the

G. Buzsáki et al. (Eds.)
Temporal Coding in the Brain

CNS is a "reality"-emulating system (Llinás and Ribary 1993a) and the parameters of such "reality" are delineated by the senses (Llinás and Paré 1991). The hypothesis that the brain is a closed system follows from the observation that the thalamic input from the cortex is larger than that from the peripheral sensory system (Wilson et al. 1984), suggesting thalamocortical iterative activity is important to brain function. Thus, thalamocortical connectivity is for the most part organized in a recurrent mode (Edelman 1987). In addition, neurons with intrinsic oscillatory capabilities that reside in this complex synaptic network allow the brain to self-generate dynamic oscillatory states which shape the computational events elicited by sensory stimuli. In this context, functional states such as wakefulness or REM sleep and other sleep stages are prominent examples of the breadth of variation that self-generated brain activity will yield.

Results of neuropsychological studies lend support to the concept of the brain as a closed system in which the role of sensory input – although absolutely essential to CNS functioning – is weighted toward the specification of internal states rather than the supply of information. The significance of sensory cues is seen mainly in their incorporation into larger cognitive entities, as adduced by reports of prosopagnosic patients who dream of faceless characters (Llinás and Paré 1991). In other words, sensory cues earn representation via their impact upon the pre-existing functional disposition of the brain.

The above hypothesis assumes that for the most part the connectivity of the human brain is present at birth and "fine-tuned" during normal maturation. This view of an *a priori* connectivity was suggested in early neurological research (Cajal 1929; Harris 1987), with the identification by Broca of a cortical speech center and the discovery of point-to-point somatotopic maps in the motor and sensory cortices (Penfield and Rasmussen 1950) and in the thalamus (Mountcastle and Henneman 1949, 1952).

A second organizing principle may be equally important – one that is based on the temporal rather then the spatial relationships among neurons. This temporal mapping may be viewed as a type of functional geometry (Pellionisz and Llinás 1982). This mechanism has been difficult to study until recently since it requires the simultaneous measurement of activity from large numbers of neurons and is not a parameter usually considered in neuroscience.

Temporal Mapping – 40-Hz Activity and Cognitive Conjunction

Synchronous neuronal activation during sensory input has recently been studied in the mammalian cerebral cortex. Synchronous activity has been recorded from cells in a given column of visual cortical cells when light bars of optimal orientation and displacement rate are presented (Eckhorn et al. 1988; Gray et al. 1989; Gray and Singer 1989). Furthermore, the components of a visual stimulus corresponding to a singular cognitive object, e.g. a line in a visual field, yield coherent 40-Hz oscillations in regions of the cortex that may be as far as 7 mm (Gray et al. 1989; Gray and Singer 1989; Singer 1993) apart, or

may even be in the contralateral cortex. In fact, 40-Hz oscillatory activity between related cortical columns has a high correlation coefficient under such circumstances. Numerous theoretical papers presenting the view that temporal mapping is integral to nervous-system function have followed from these findings.

The central tenet of the temporal mapping hypothesis can be summarized simply. Spatial mapping creates a finite universe of possible representations. The addition of a second component capable of generating new combinations of such spatial mapping by means of temporal conjunction generates an immensely larger set of representations as categorization is achieved by the superposition of spatial and temporal mapping via thalamocortical resonant iteration.

MEG Studies

The presence of continuous and coherent 40-Hz oscillations throughout the cortical mantle of awake human subjects has been revealed by magnetoencephalography (MEG); (Llinás and Ribary 1992). These oscillations may be reset by sensory stimuli, and phase comparison revealed the presence of a 12- to 13-msec phase shift between the rostral and caudal poles of the brain (Llinás and Ribary 1992). The 40-Hz oscillation displays a high degree of spatial organization and thus may be a candidate mechanism for the production of temporal conjunction of rhythmic activity over a large ensemble of neurons.

The mechanism by which 40-Hz oscillation may be generated has been studied at the level of single neurons and that of neuronal circuits. For example, it has been shown that the membrane potential of sparsely spiny inhibitory neurons in cortical layer IV supports 40-Hz activity (Fig. 1); the mechanism for the oscillation being a sequential activation of a persistent low-threshold sodium current (Llinás and Sugimori 1980) followed by a subsequent potassium conductance (Llinás et al. 1991). The inhibitory input of these sparsely spinous interneurons onto pyramidal cells projecting to the thalamus can entrain 40-Hz oscillation in the reticular nucleus and so entrain, by rebound activation, the specific and nonspecific thalamus. This issue will be treated in the modeling part of this paper. Indeed, since the GABAergic reticular thalamic neurons project to most of the relay nuclei of the thalamus (Steriade et al. 1984), layer-IV cells would indirectly make a contribution to the 40-Hz resonant oscillation in the thalamocortical network. It has recently been demonstrated that under *in vivo* conditions relay-thalamic and reticular-nucleus neurons and pyramidal cells themselves are capable of 40-Hz oscillation on their own, laying out in this manner the possibility for network resonance intrinsically at 40 Hz (Steriade et al. 1993). The ionic mechanisms underlying this oscillation are similar to those of the spiny layer-IV neurons (Steriade et al. 1991).

When the interconnectivity of these nuclei is combined with the intrinsic properties of the individual neurons, a network for resonant neuronal oscil-

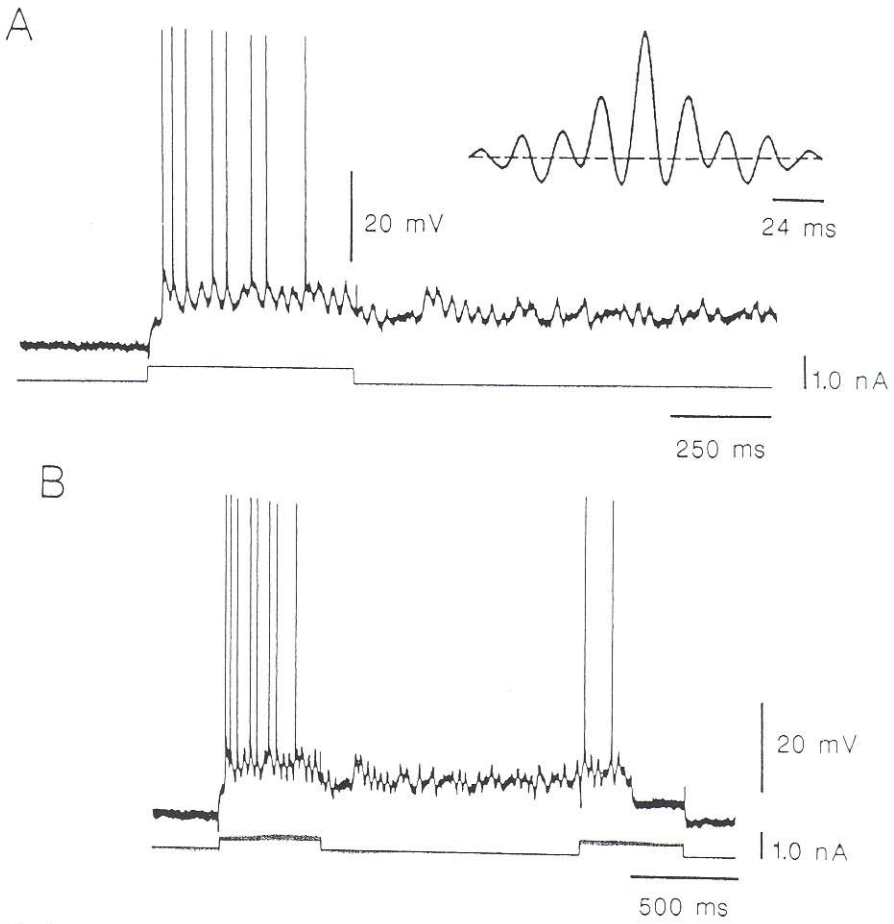

Fig. 1. *In vitro* intracellular recording from a sparsely spinous neuron of the fourth layer of the frontal cortex of guinea pig. **A** The characteristic response obtained in the cell, following direct depolarization, consisting of a sustained subthreshold oscillatory activity on which single spikes can be observed. The intrinsic oscillatory frequency was 42 Hz, as demonstrated by the auto-correlogram shown in the upper right corner. **B** The same record as in **A** but at slower sweep speed, demonstrating how the response outlasts the first stimuli but comes to an abrupt cessation in the middle of a second stimulus. (Modified from Llinás et al. 1991)

lation emerges in which specific cortico-thalamo-cortical circuits would tend to resonate at 40 Hz. According to this hypothesis neurons at the different levels, and most particularly those in the reticular nucleus, would be responsible for the synchronization of 40-Hz oscillation in distant thalamic and cortical sites. As we will see later, these oscillations may be organized globally over the CNS, especially as it has been shown that neighboring reticular-nucleus cells are linked by dendro-dendritic and intranuclear axon collaterals (Deschênes et al. 1985; Yen et al. 1985).

Thalamocortical Resonance and the Functional Basis for Consciousness

If we surmise that the rostrocaudal 40-Hz phase shift observed in our studies and the coherent waves that scan the brain at 40 Hz are related, we may conclude that consciousness is a noncontinuous event determined by the simultaneity of activity in the thalamocortical system. Since this resonance is present during REM sleep (Llinás and Ribary 1993b) but is not seen during non-REM sleep, we may postulate further that the resonance is modulated by the brainstem and would be given content by sensory input in the awake state and by intrinsic activity during dreaming.

Proceeding with this train of thought we would assume that state-dependent fluctuations of the membrane potential of thalamic neurons result from the resonant interactions between synaptic input extrinsic to the thalamocortical circuit. The firing mode of these cells, which ultimately is cognition, relates to their intrinsic membrane properties and their thalamocortical interconnectivity. If this is indeed the case, then, sensory input during REM sleep that is not correlated temporally with ongoing thalamocortical activity (i.e., is not put into the context of thalamocortical "reality") does not exist as a functionally meaningful event.

On the other hand, if the responsiveness generated during the waking state is duplicated in the absence of the appropriate sensory input by virtue of activity generated via thalamocortical interactions, reality-emulating states such as hallucinations may be generated. The implications of this proposal are of some consequence, for if consciousness is a product of thalamocortical activity, it is the dialogue between the thalamus and the cortex that generates subjectivity.

Based on the above argument we have proposed that the perception of external reality is an intrinsic function of the CNS, developed and honed by the same evolutionary pressures that generated other specializations. Indeed, the major development in the evolution of the brain of higher primates, including man, is enrichment of the corticothalamic system. Evolutionary studies show that the surface area of the neocortex in man is approximately three times that of higher apes (Lande 1979).

Moreover, this hypothesis implies that secondary qualities of our senses such as colors, identified smells, tastes and sounds are inventions of the CNS that allow the brain to interact with the external world in a predictive manner (Llinás 1987). The degree to which our perception of reality and "actual" reality overlap is inconsequential as long as the predictive properties of the computational states generated by the brain meet the requirements for successful interactions with the external world.

Similarities Between REM Sleep and Wakefulness

A role for 40-Hz thalamocortical resonance within the global temporal mapping, which we propose generates cognition, is supported by recent magneto-

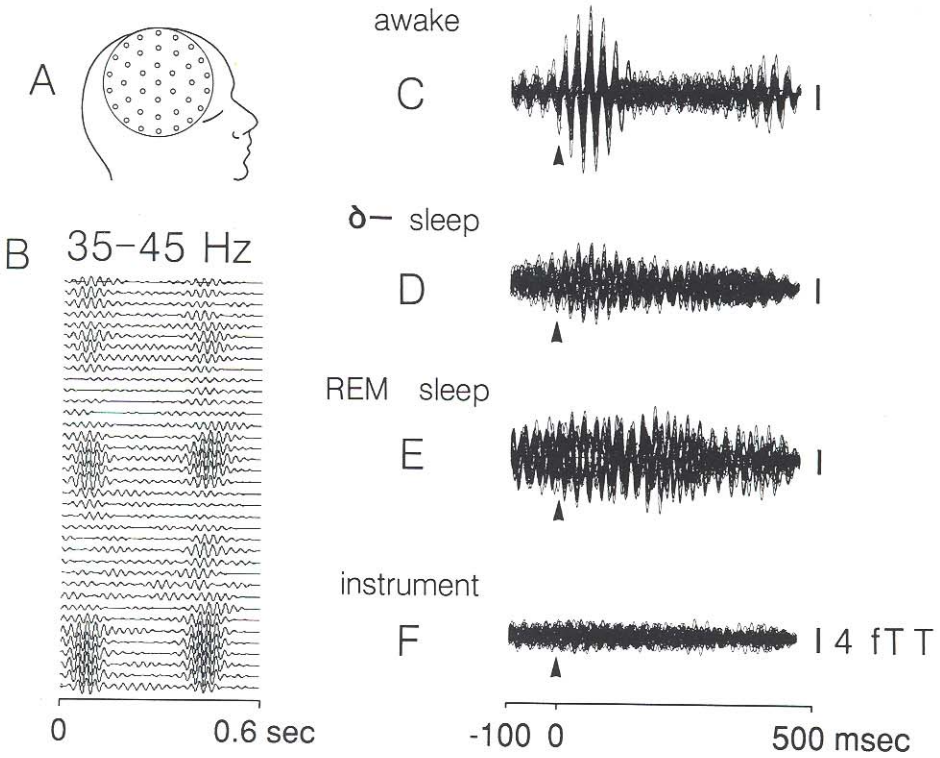

Fig. 2. 40-Hz oscillation in wakefulness and a lack of 40-Hz reset in delta sleep and REM sleep. Recording using a 37-channel MEG. (**A**) Diagram of sensor distribution over the head and in (**B**) the spontaneous magnetic recordings from the 37 sensors during wakefulness are shown immediately below (filtered at 35–45 Hz). In (**C–F**) averaged oscillatory responses (300 epochs) following auditory stimulus. In **C**, the subject is awake and the stimulus is followed by a reset of 40-Hz activity. In **D** and **E**, the stimulus produced no resetting of the rhythm. (**F**) The noise of the system in femtotesla (fT). (Modified from Llinás and Ribary 1993)

encephalography studies showing the presence of organized 40-Hz activity with a rostrocaudal phase shift during REM sleep (Llinás and Ribary 1993b).

These studies addressed issues concerning 1) the presence of 40-Hz activity during sleep, 2) the possible differences between 40-Hz resetting in different sleep/wakefulness states and, 3) the question of 40-Hz scan during REM sleep.

Spontaneous magnetic activity was recorded continuously during wakefulness, delta sleep and REM sleep using a 37-channel sensor array positioned as shown in Figure 2A. Since Fourier analysis of the spontaneous, broadly filtered rhythmicity (1–200 Hz) demonstrated a large peak of activity at 40 Hz over much of the cortex, we decided that it was permissible to filter the data at 35–45 Hz. Large coherent signals with a high signal-to-noise ratio were typically recorded from all 37 sensors as shown in Figure 2B, for a single 0.6-sec epoch of global spontaneous oscillations in an awake individual.

The second set of experiments examined the responsiveness of the oscillation to an auditory stimulus during wakefulness, delta sleep and REM sleep. Tthe stimulus comprised frequency-modulated 500-msec tone bins, triggered 100 msec after the onset of the 600-msec recording epoch; recordings were made at random intervals over about 10 minutes. In agreement with previous findings (Ribary et al. 1991; Galambos et al. 1981; Pantev et al. 1991), auditory stimuli produced well-defined 40-Hz oscillation during wakefulness (Fig. 2C), but no resetting was observed during delta (Fig. 2D) or REM sleep (Fig. 2E) in this subject or the six other subjects examined (Llinás and Ribary 1993b).

The traces in Figure 2C–F are a superposition of the 37 traces recorded during a 600-msec epoch. Their alignment in panel C indicates the high level of coherence of the 40-Hz activity at all the recording points following the auditory stimulus.

These findings indicated that, whereas the awake state and the REM sleep state are electrically similar with respect to the presence of 40-Hz oscillations, a central difference remains, that of the inability of sensory input to reset the 40-Hz activity during REM sleep. By contrast, during delta sleep the amplitude of these oscillators differs from that of wakefulness and REM sleep but, as in REM sleep, there is no 40-Hz sensory response.

While wakefulness and REM sleep can both generate cognitive experiences, the above findings corroborate what is commonly known – that the external environment is for the most part excluded from the imaging that is characteristic of the oneiric states. This further substantiates a recent proposal (Llinás and Paré 1991) that the dreaming brain is characterized by an increased attentiveness to its intrinsic state and that external stimuli do not perturb this activity.

While there is coherence among the different recording sites as shown in Figure 2, there is also a phase shift of the oscillation along the different sites (Llinás and Ribary 1992), as shown in Figure 3. Spontaneous 40-Hz activity during a single, 0.6-sec epoch recorded during REM sleep is shown in Figure 3A. The well-organized 12-msec phase shift of this 40-Hz burst of activity is shown in panel B, where a portion of each of five traces recorded from the locations diagrammed in panel C is expanded. The 37 recording sites are shown in panel D. Although a similar 12-msec phase shift was observed in this individual in the awake state, the rostrocaudal sweep was not as well organized or as repeatable as that seen during REM sleep, probably because in the awake state the sweep is continually reset by incoming sensory stimuli.

The significant new finding here is the presence of 40-Hz oscillation during REM sleep that demonstrates a similar distribution, phase, and amplitude to that observed during wakefulness. The overall speed of the rostrocaudal scan in the five individuals studied averaged near 12.5 milliseconds, corresponding quite closely to half a 40-Hz period. This number is the same as that calculated by Kristofferson (1984) for a quantum of consciousness in his psychophysical studies in the auditory system.

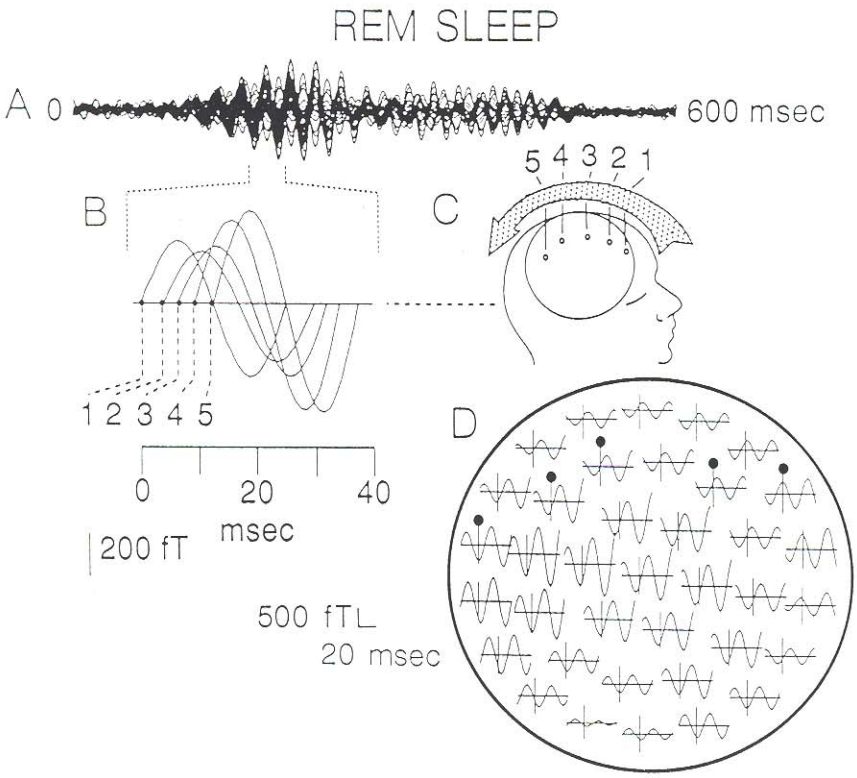

Fig. 3. Rostrocaudal phase shift of 40 Hz during REM sleep as measured using MEG (see also Fig. 2). The upper trace (**A**) shows synchronous activation in all 37 channels during a 600-msec period. The oscillation in the left part of trace **A** has been expanded in trace **B** to show five different recording sites over the head. The five recording sites of trace **B** are displayed in diagram **C** for a single epoch, to demonstrate the phase shift for the different 40-Hz waves during REM sleep. The direction of the phase shift is illustrated by an arrow above diagram **C**. The actual traces and their site of recordings for a single epoch are illustrated in diagram **D** for all 37 channels, fT, femtotesla. (Modified from Llinás and Ribary 1993)

A second significant findings is that 40-Hz oscillations are not reset by sensory input during REM sleep, although clear evoked-potential responses indicate that the thalamo-neocortical system is accessible to sensory input (Llinás and Paré 1991; Steriade 1991). We consider this to be the central difference between dreaming and wakefulness. These data suggest that we do not perceive the external world during REM sleep because the intrinsic activity of the nervous system does not place sensory input in the context of the functional state being generated by the brain (Llinás and Paré 1991). That is, the dreaming condition is a state of hyperattentiveness to intrinsic activity in which sensory input cannot access the machinery that generates conscious experience.

An attractive possibility in considering the morphophysiological substrate is that the "nonspecific" thalamic system, particularly the intralaminar complex, plays an important part in the scanning. Indeed, neurons in this complex project in a spatially continuous manner to the most superficial layers of all cortical areas, including the primary sensory cortices. This group of cells may also have the necessary interconnectivity to sustain an intranuclear propagation wave resulting in the 40-Hz phase shift seen at the cortical level as a rostrocaudal 12.5-msec phase-shift. This possibility is particularly attractive given that single neurons burst at 30–40-Hz (Steriade et al. 1993) especially during REM sleep, which is a finding consistent with the macroscopic magnetic recordings observed in this study, and given that damage of the intralaminar system results in lethargy (Facon et al. 1958; Castaigne et al. 1962), while unilateral lesions result in hemineglect (Heilman and Balenstein 1993).

Binding and Specific and Nonspecific 40-Hz Resonant Conjunctions: The Issue of Coincidence Detection

The results reported above and other recent findings indicate that 40-Hz oscillations are present at many levels in the CNS including the retina (Ghose and Freeman 1992), olfactory bulb (Bressler and Freeman 1980), specific and nonspecific, thalamic nuclei, (Steriade et al. 1993), reticular nucleus (Pinault and Deschênes 1992), and neocortex (Llinás et al. 1991). Some of the 40-Hz activity recorded in the visual cortex is correlated with 40-Hz activity in the retina (Ghose and Freeman 1992). A scheme through which the correlation of thalamic and cortical 40-Hz oscillation may subserve temporal binding is presented on the left side of Figure 4. Forty-Hz oscillations in neurons in specific thalamic nuclei (Steriade et al. 1990) establish cortical resonance through direct activation of pyramidal cells and feed forward inhibition through activation of 40-Hz inhibitory interneurons in layer IV (Llinás et al. 1991). These oscillations re-enter the thalamus via layer-VI pyramical-cell axon collaterals (Steriade et al. 1990), producing thalamic feedback inhibition via the reticular nucleus (Steriade et al. 1984). This view differs from the binding hypothesis proposed by Crick and Koch (1990), in which cortical binding is attributed to the activation of cortical V4, pulvinar or claustrum.

A second system is illustrated on the right side of Figure 4. Here the intralaminar nonspecific thalamic nuclei projection to cortical layers I and V and to the reticular nucleus (Penfield and Rasmussen 1950), is illustrated. Layer V pyramidal cells return oscillations to the reticular nucleus and intralaminar nuclei. The cells in this complex have been shown to oscillate in 40-Hz bursts (Steriade et al. 1993) and to be organized macroscopically as a toroidal mass input having the possibility of recursive activation (Krieg 1966). This could result in the recurrent activity ultimately responsible for the rostrocaudal cortical activation found in the present MEG recordings.

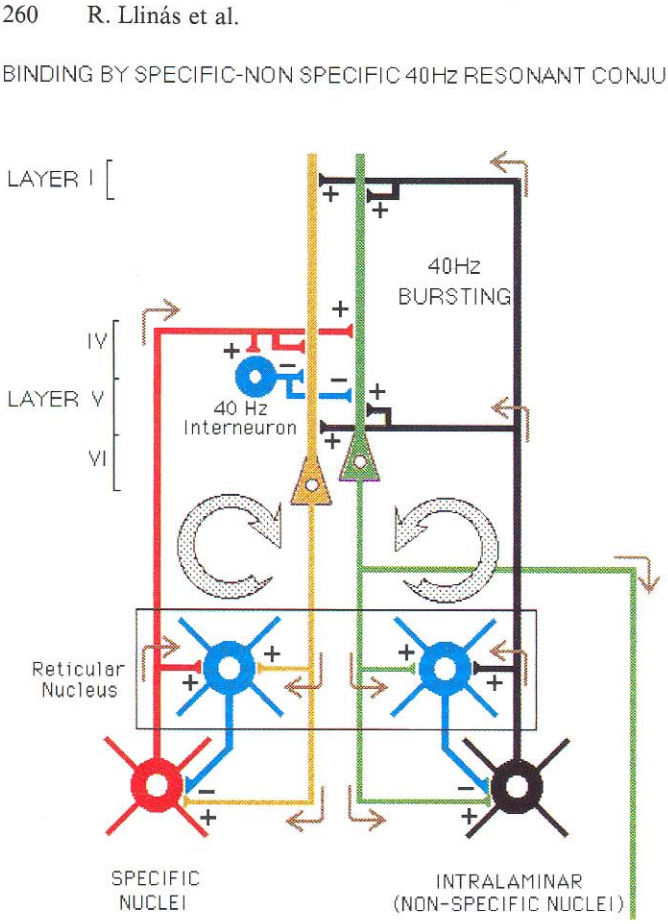

Fig. 4. Thalamocortical circuits proposed to subserve temporal binding. Diagram of two thalamocortical systems. *Left* Specific sensory or motor nuclei project to layer IV of the cortex, producing cortical oscillation by direct activation and feed-forward inhibition via 40-Hz inhibitory interneurons. Collaterals of these projections produce thalamic fedback inhibition via the reticular nucleus. The return pathway (circular arrow on the right) re-enters this oscillation to specific and reticularis thalamic nuclei via layer VI pyramidal cells. *Right* Second loop shows nonspecific intralaminary nuclei projecting to the most superficial layer of the cortex and giving collaterals to the reticular nucleus. Layer V pyramidal cells return oscillation to the reticular and the nonspecific thalamic nuclei, establishing a second resonant loop. The conjunction of the specific and nonspecific loops is proposed to generate temporal binding. (Modified from Llinás and Ribary 1993a)

It is also evident from the literature that neither of these two circuits alone can generate cognition. Indeed, as stated above, damage of the nonspecific thalamus produces deep disturbances of consciousness while damage of specific systems produces loss of the particular modality. Although at this early stage it must be quite simple in its form, the above finding suggests a hypothesis regarding the overall organization of brain function. This rests on two

tenets. First, the "specific" thalamocortical system is viewed as encoding specific sensory and motor "information" by the resonant thalamocortical system specialized to receive such inputs (e. g., the LGN and visual cortex). The specific system is understood to comprise those nuclei, whether sensorimotor or associative, that project mainly, if not exclusively, to layer IV in the cortex. Second, following optimal activation, any such thalamocortical loop would tend to oscillate near 40-Hz and activity in the "specific" thalamocortical system could be easily "recognized" over the cortex by this oscillatory characteristic.

In this scheme, areas of cortical sites "peaking" at 40-Hz would represent the different components of the cognitive world that have reached optimal activity at that time. The problem now is the conjunction of such a fractured description into a single cognitive event. We propose that this could come about by the concurrent summation of specific and nonspecific 40-Hz activity along the radial dendritic axis of given cortical elements, that is, by the superposition of spatial and temporal mapping, i.e., by coincidence detection.

In short, the system would function by inciting central neurons to optimal firing patterns via integrations based on passive and active dendritic conduction along the apical dendritic core conductors. In this way, the time-coherent activity of the specific and nonspecific oscillatory inputs, by summing distal and proximal activity in given dendritic elements, would enhance *de facto* 40-Hz cortical coherence by their multimodal character and thereby would provide one mechanism for global binding. The "specific" system would thus provide the *content* that relates to the external world and the nonspecific system would give rise to the temporal conjunction, or the *context* (on the basis of a more interoceptive context concerned with alertness), that would together generate a single cognitive experience.

Modeling Coincidence Interaction Between Specific and Nonspecific Thalamic Nuclei and the Overlying Cerebral Cortex

Based on the above, as well as previous findings (Wang 1993), we have proposed that the binding of sensory information into a single cognitive state is implemented through the temporal coherence of inputs from specific and nonspecific thalamic nuclei at the cortical level (Llinás and Ribary 1993b). Furthermore, we consider this coincidence detection the basis of temporal binding. To help develop this hypothesis we have implemented a mathematical model of a four-neuron thalamocortical circuit that would provide a first-order approximation of the proposed binding circuit.

In this simplified network model, specific thalamic inputs are represented by a thalamic neuron (Fig. 5, STC, red) that projects to cortical layer IV after sending an axon collateral to the reticular nucleus (Fig. 5, RTC, blue). Intralaminar, nonspecific thalamic inputs are represented by a second neuron (Fig. 5,

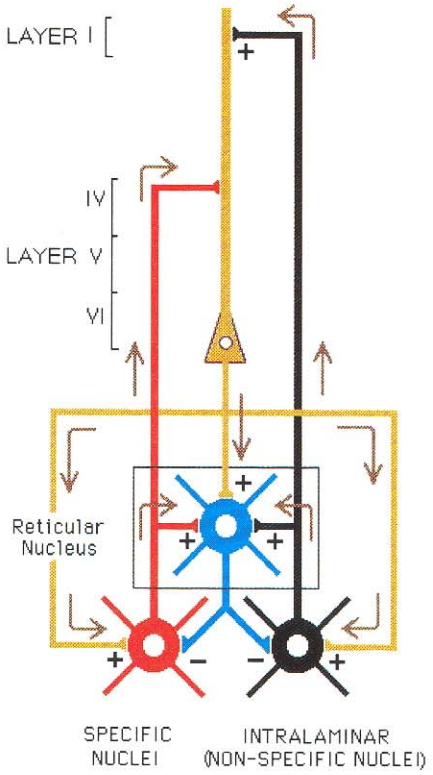

Fig. 5. Schematic wiring diagram for our four-cell network model. STC, specific thalamic cell; ITC, intralaminar thalamic cell; RTC, reticular nucleus cell; PC, (cortical) pyramidal cell. Only one PC was included here. In this modeling, each element was described as a point cell and each possessed the Hodgkin-Huxley type of ion current for action-potential generation. The SC, ITC and RTC – but not the PC – were endowed with a persistent sodium current and a slowly inactivating potassium current that enabled them to oscillate at 30–50 Hz under appropriate depolarization

ITC, black) that projects to cortical layer I after sending axon collaterals to the reticular nucleus. The reticular nucleus neuron is the third cell (Fig. 5, RTC, blue); it sends an inhibitory projection to specific and interlaminary nuclear cells. The pyramidal cells in layers I and V are modeled by a single neuron (Fig. 5, yellow) that receives inputs and projects to both specific (red) and nonspecific (black) thalamic neurons and gives axon collaterals to the reticular nucleus (blue). The cortical inhibitory interneuron will be added to this circuit at the next stage of this model.

The membrane properties of the model cells were based on the interplay between a persistent sodium conductance (g_{NaP}) and a slowly inactivating potassium conductance (g_{KS}). These conductances can be activated in the subthreshold-depolarizing range of membrane potential and have been shown to enable a single cell to oscillate at 30–50 Hz with appropriate depolarization (Wang 1993). As suggested by experimental evidence (Llinás and Ribary 1992; Steriade et al. 1993; Pinault and Deschênes 1992), the model specific-thalamic, intralaminar and reticular nucleus cell types have these conductances; the intralaminar cell has the strongest intrinsic 40-Hz rhythmicity.

Excitatory postsynaptic potentials elicited by activity in specific thalamic or intralaminar cells are mediated by non-NMDA (AMPA) glutamate recep-

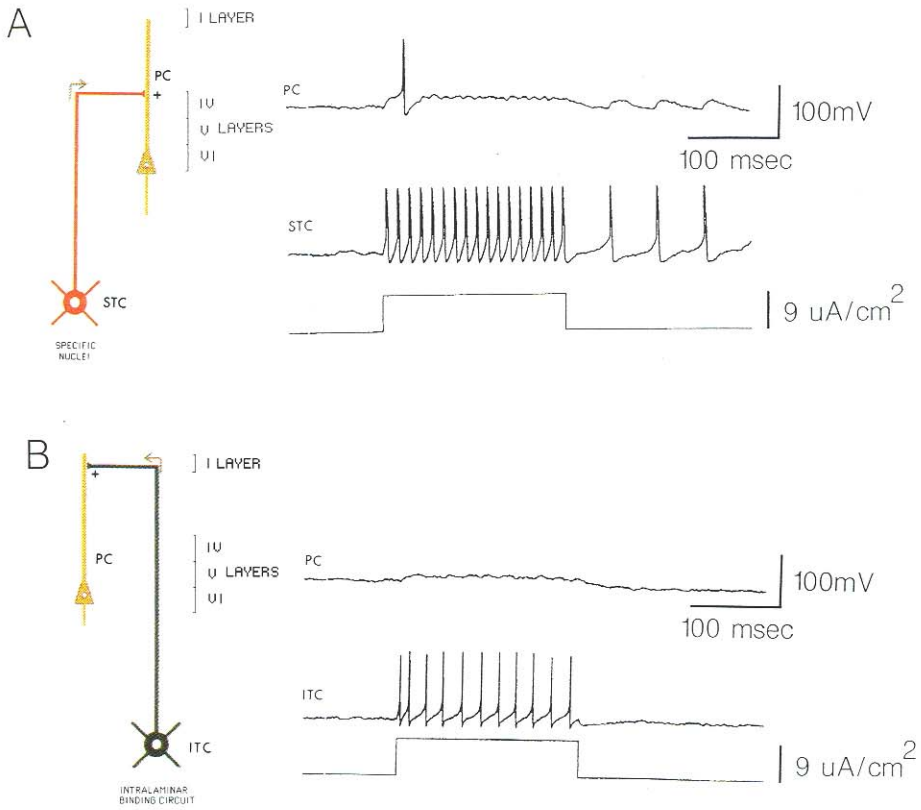

Fig. 6. Isolated specific (**A**) or nonspecific (**B**) thalamocortical pathway; stimulation of STC (**A**) of ITC (**B**) by a 200-msec current pulse induced a train of action potentials in this cell. The cortical PC, however, only displayed synaptic depolarization of small amplitude

tors in the model. Inhibitory postsynaptic potentials due to reticular-nucleus cell activity are mediated by $GABA_A$ receptors. $GABA_B$ receptors are also present in these cells but are not included in this model. Model pyramidal cells fire tonic spike trains upon sufficient depolarization. Pyramidal cell corticofugal excitation is mediated by NMDA-type glutamate receptors in this model (see below for explanation).

The simulations presented in Figures 6–8 illustrate three aspects of the thalamocortical resonance hypothesis put forth in this paper. First, the reticular neuron is essential for the organization of thalamocortical resonance. Second, the pyramidal cell behaves as a coincidence detector for simultaneity of activity in the specific and intralaminary afferent systems. Third, the corticofugal pathway is essential for maintaining oscillatory activity.

For ease of description the model is presented in four steps. The first examines the properties of the model comprising two neurons; the specific thalamic cell and a pyramidal cell (Fig. 6A), or the intralaminar neuron and

the pyramidal cell (Fig. 6B). Under these conditions, injection of a 200-msec current pulse into the soma of the specific thalamic cell (STC) elicited tonic firing during the pulse that continued at a lower frequency after the pulse. A single spike and low-amplitude oscillations were seen in the pyramidal cell (PC) during the pulse while EPSPs were correlated with the STC post-pulse spikes (Fig. 6A).

When the intralaminar cell (ITC) was activated, a train of spikes was evoked in this element (Fig. 6B) and subthreshold oscillations were synaptically elicited in the pyramidal cell, but there was no spike activity. In both cases the thalamocortical synapse was weighted to elicit only subthreshold responses in the pyramidal cell.

The second step was to add the reticular nucleus cell (RTC) to the circuit, as shown in Figure 7, excluding the corticothalamic pathway. In this case, current injection into the specific nucleus and the intralaminar nucleus elicited a few spikes and an epoch of subthreshold oscillations in STC (Fig. 7A, STC). In this simulation the persistent sodium conductance in STC was blocked and the subthreshold oscillatory fluctuations were due to the IPSPs from the reticular nucleus neurons rather than intrinsic membrane properties. Firing of the two types of thalamic cell elicited spikes in the cortical pyramidal cell (Fig. 7A, PC) while the ITC fired repetitively, as did the RTC. Note that the spikes in the PC occur reliably when the specific thalamic input and the intralaminar input coincided in time.

The third step was to include the corticothalamic return pathway and to determine its effect on the dynamics of the model circuit under these new conditions (Fig. 8A). If the specific thalamic nuclear cell was activated with a current pulse, a few spikes were elicited followed by an epoch of subthreshold oscillations that are due to sequential activation of g_{NAP} and g_{KS} and are modulated by synaptic inputs from the reticular nucleus cell. This intrinsically generated subthreshold oscillation is not correlated closely with the firing in RTC, unlike in Fig. 7 where the persistent sodium conductance in STC was blocked and the small oscillations were IPSP events. The single spike seen in the pyramical cell was elicited spontaneously by summation of noise and by the thalamic synaptic depolarization (Fig. 8B). The PC spike, in turn, generated excitation in the reticular and intralaminar cells via the corticofugal projection. The effect of pyramidal excitation is long-lasting because of the slow decay of the NMDA-type postsynaptic potential ($t = 40$ msec) and is responsible for eliciting, for instance, the double spikes in the ITC (Fig. 8B, ITC). When the nonspecific ITC alone was stimulated (Fig. 8C, STC), the ITC oscillated at about 35-Hz, accompanied by action potentials at the peak of each oscillatory event (Fig. 8C). Under the influence of subthreshold synaptic excitations from the ITC, the PC fired a single spike which induced a spike in the STC. Therefore, the cortical PC remained essentially quiet in both cases of Figure 8B and C. In fact, the synaptic weights were tuned such that neither the specific thalamic nor the intralaminar projection alone could efficiently activate the cortical PC.

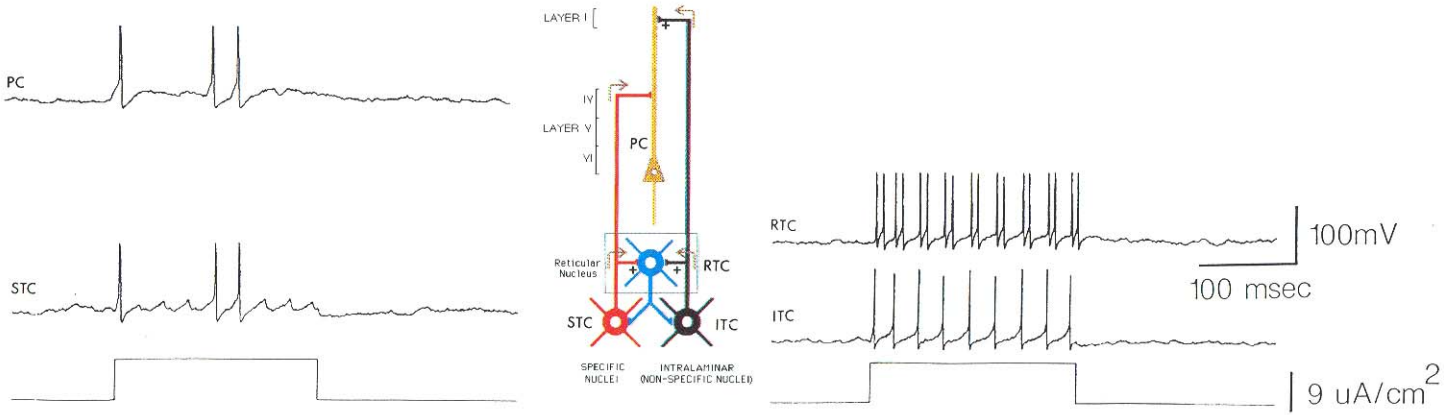

Fig. 7. Coactivation of the specific and nonspecific thalamic pathways in the absence of the corticofugal return projection. An identical current pulse was applied simultaneously to STC and ITC. In this simulation the recurrent inhibition from RTC had relatively strong synaptic weights. In particular, it suppressed many of the spikes in STC. The persistent sodium conductance in STC was blocked in this simulation. The cortical PC emitted spikes only when both STC and ITC were firing simultaneously

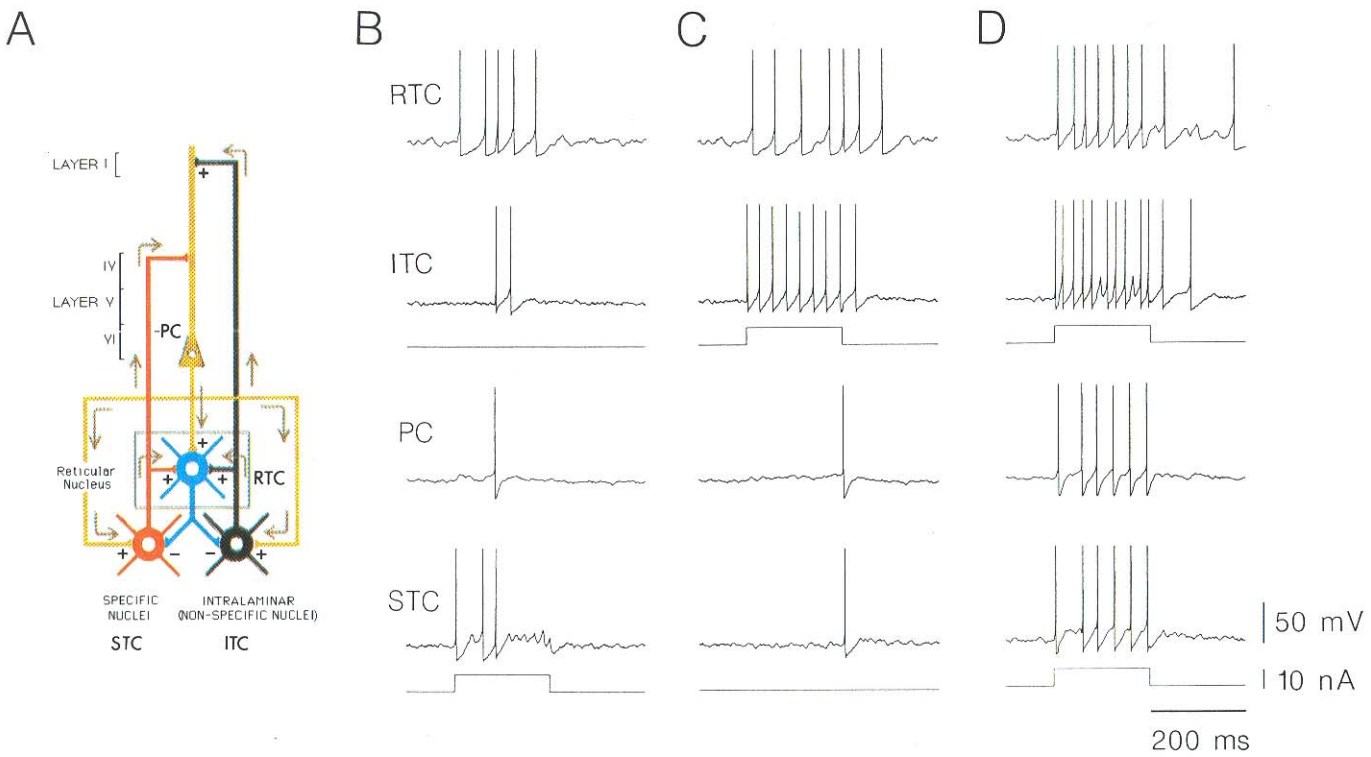

Fig. 8. Full thalamocortical circuit as shown in Fig. 5. **A** Complete circuit diagram as in Figure 5. **A** 200-msec current pulse was applied to either STC (**B**) or ITC (**C**). In **B** STC displayed a few spikes followed by an epoch of subthreshold oscillations. These latter were produced not by synaptic inputs (in contrast in Fig. 7) but by intrinsic membrane properties. In **C**, ITC displayed a regular oscillation of action potentials. In either case PC remained essentially at rest. Hence, even in the completed circuit, the activation of either the specific or nonspecific thalamic afferent system alone could not activate the cortical PC. In **D**, with coincident activation of STC and ITC, the cortical PC was now induced to fire regular spikes at about 35 Hz. Its firing was closely matched with that of the STC, whereas the ITC had a significantly higher firing rate

The fourth step was to use the model to begin to test our hypothesis that binding could occur at the level of the cortex through simultaneous activation of both classes of thalamic nuclear cells. In the complete ("intact") system (Fig. 8D), when both the ITC and STC are activated, the PC fired at about 30 Hz, in close synchrony with the STC. The ITC had a significantly higher firing rate, near 50 Hz. Note that the recurrent inhibition from the RTC also had a rhythmic component due to its intrinsic membrane properties. It subserves to regulate the excitability of the STC and ITC. The completed circuit displays a tendency to oscillate coherently for some time, until the event disappears due to the drive reduction to the thalamic nuclei.

It is of interest to note again the importance of utilizing the NMDA-type glutamate-receptor synapses for the corticothalamic projections. Indeed, from the assumption that the PC is a coincidence detector, it follows that this cell cannot fire at a higher rate than the STC. If the firing of the latter is low in the absence of the corticofugal input, activity of the PC would not be able to increase thalamic firing rate *if* the feedback synapses were fast (of the AMPA type with a decay time of less than 10 msec). This limitation is overcome when the corticofugal excitation can persist for some time. The NMDA-type corticothalamic synapses, which are known to exist (Deschênes and Hu 1990; Scharfman et al. 1990), were used in our model for this particular purpose.

To conclude, then, the point to be made here is that the optimally organized 40-Hz resonance in the thalamocortical circuit requires a coactivation of the specific and the nonspecific systems as well as the corticofugal projection. The impairment of either of these would be detrimental to the normal function of the thalamocortical system during arousal and cognitive processes.

Appendix

In this appendix, we describe in detail our four-cell model. We shall first discuss the intrinsic ion currents and synaptic currents. The circuit equations for the model will then be presented, together with the parameter values.

Ionic Currents

The model made use of the Hodgkin-Huxley type spike generating currents (I_{Na} and I_K), a persistent sodium current (I_{NaP}), a slowly inactivating potassium current (I_{KS}), a T-type calcium current (I_T) and an A-type potassium current (I_A).

I_{Na} and I_K. Let $I_{Na} = g_{Na} m_\infty^p(V)\, h(V - V_{Na})$, $I_K = g_K n^q (V - V_K)$, with $V_{Na} = +55$ mV, $V_K = -90$ mV. The activation of I_{Na} being fast, the variable m was replaced by its steady state function m_∞. The other two gating variables h and n obey a kinetic equation of the form

$$\frac{d\chi}{dt} = \alpha_\chi(V)(1-\chi) - \beta_\chi(V)\chi = (\chi_\infty(V) - \chi)/\tau_\chi(V). \tag{1}$$

We have used three different variants of the Hodgkin-Huxley currents. The parameter σ below is used for fine tuning the action potential threshold.

The Hodgkin-Huxley (HH) expression (Hodgkin and Huxley 1952) assumes $p = 3$ and $q = 4$. $\alpha_m = -0.1(V + 30 - \sigma)/(\exp(-0.1(V + 30 - \sigma)) - 1)$, $\beta_m = 4\exp(-(V + 55 - \sigma)/18)$; $\alpha_h = 0.07\exp(-(V + 44 - \sigma)/20)$, $\beta_h = 1/(\exp \cdot (-0.1(V + 14 - \sigma)) + 1)$; $\alpha_n = -0.01(V + 34 - \sigma)/(\exp(-0.1(V + 34 - \sigma)) - 1)$, and $\beta_n = 0.125\exp(-(V + 44 - \sigma)/80)$. In order to incorporate a temperature correction, we divided α_h, β_h, α_n and β_n by a factor of 0.35.

The Traub (T) expressions (Traub 1977) was modified from the HH formulation in order to model spike discharges at very high rate (up to 1000 Hz) in the Renshaw motoneurons. We have $p = 3$, $q = 4$. $\alpha_m = -0.8(V + 37.5 - \sigma)/(\exp(-(V + 37.5 - \sigma)/4) - 1)$, $\beta_m = 0.7(V + 10 - \sigma)/(\exp((V + 10 - \sigma)/5) - 1)$; $\alpha_h = 0.32\exp(-(V + 25 - \sigma)/18)$, $\beta_h = 10/(\exp(-(V + 10 - \sigma)/5) + 1)$; $\alpha_n = -0.03(V + 35 - \sigma)/(\exp(-(V + 35 - \sigma)/5) - 1)$, and $\beta_n = 0.5\exp(-(V + 40 - \sigma)/40)$.

The Traub-Wong-Miles-Michelson (TWMM) expression (Traub et al. 1991) was based on voltage-clamp data from hippocampal pyramidal cells, and is probably more adequate for modeling the cortical cells than the other two expressions. We have $p = 2$, $q = 1$. $\alpha_m = -0.32(V + 46.9 - \sigma)/(\exp(-(V + 46.9 - \sigma)/4) - 1)$, $\beta_m = 0.28(V + 19.9 - \sigma)/(\exp(-(V + 19.9 - \sigma)/5) - 1)$; $\alpha_h = 0.128\exp(-(V + 43 - \sigma)/18)$, $\beta_h = 4/(\exp(-(V + 20 - \sigma)/5) + 1)$; $\alpha_n = -0.016(V + 24.9 - \sigma)/(\exp(-(V + 24.9 - \sigma)/5) - 1)$, and $\beta_n = 0.25\exp(-(V + 40 - \sigma)/40)$.

I_{NaP} and I_{KS}. These are two voltage-dependent currents which are activated in the subthreshold depolarizing range (Wang 1993). The persistent sodium current $I_{NaP} = g_{NaP} m_\infty(V)(V - V_{Na})$, with $m_\infty = 1/(1 + \exp(-(V + 51)/5))$.

The slowly inactivating potassium current $I_{KS} = g_{KS} m(\varrho h_1 + (1 - \varrho)h_2)(V - V_K)$, with two components of the respective fractions $\varrho = 0.6$ and $(1 - \varrho) = 0.4$. We have $m_\infty = 1/(1 + \exp(-(V + 34)/6.5))$, and τ_m is assumed to be independent of the voltage. This activation time constant have not been accurately measured, its estimated range is 5 to 20 msec. the two inactivation variables h_1 and h_2 have a same steady-state function, $h_\infty = 1/(1 + \exp((V + 65)/6.6))$, but disparate time constants: $\tau_{h1} = 200 + 220/(1 + \exp(-(V + 71.6)/6.85))$, and $\tau_{h2} = 200 + 3200/(1 + \exp(-(V + 63.6)/4))$.

I_T and I_A. These two currents share a common property that they require hyperpolarization to be de-inactivated. They were occasionally included in the simulations, but did not play a crucial role in our model. The T-type calcium current is taken from Ref. 47: $I_T = g_T m_\infty^3 h(V - V_{Ca})$, with $V_{Ca} = +120$ mV. $m_\infty = 1/(1 + \exp(-(V + 65)/7.8))$, $h_\infty = 1/(1 + \exp((V + 81)/5))$, $\tau_h = h_\infty(V) \cdot \exp((V + 162.3)/17.8) + 20$. The A-type potassium current is due to Connor et al. (1977), $I_A = g_A A_\infty^3(V) B(V - V_K)$, $A_\infty = \{0.0761\exp((V + 94.22)/31.84)/(1 + \exp((V + 1.17)/28.93))\}^{1/3}$, $B_\infty = 1/\{1 + \exp((V + 53.3)/14.54)\}^4$, $\tau_B = 1.24 + 2.678/(1 + \exp((V + 50)/16.027))$.

Synaptic Currents

We have modeled each synaptic current by an autonomous differential equation as follows (Wang and Rinzel 1993): $I_{syn} = g_{syn} s(V_{post} - V_{syn})$, where the gating variable s obeys the equation

$$\frac{ds}{dt} = S_\infty(V_{pres})(1 - s) - k_r s;$$

$$S_\infty(V_{pres}) = 1/(1 + \exp(-(V_{pres} + 40)/2)). \quad (2)$$

The parameter $1/k_r$ is the synaptic decay time constant. So, when the presynaptic membrane potential V_{pres} reaches a certain threshold (of action potential), $S_\infty(V_{pres})$ becomes significant, and the synaptic gating variable s increases according to Eq. (2). At the termination of the action potential, V_{pres} falls below the threshold, and $S_\infty(V_{pres})$ becomes negligeable. Then s decays to zero with a time constant $1/k_r$.

Our model included three types of synaptic currents. Two excitatory glutamate currents have the reversal potential $V_{syn} = 0$ mV. The fast (AMPA) and slow (NMDA) currents have, respectively, $1/k_r = 10$ ms and 40 ms. The fast inhibitory $GABA_A$ current has a reversal potential $V_{syn} = -75$ mV, and a time constant $1/k_r = 10$ ms.

The Model

In our model there are four neuron types: the reticular-nucleus cell (RTC), the specific thalamic relay cell (STC), the intralaminar thalamic cell (ITC), and the cortical pyramidal cell (PC). Each cell obeys a circuit equation

$$C_m \frac{dV}{dt} = -I_{NaP} - I_{KS} - I_{Na} - I_K - I_T - I_A - I_L - \sum I_{syn} + I_{app} + c\xi(t), \quad (3)$$

where $C_m = 1\,\mu F/cm^2$, $I_L = g_L(V - V_L)$ is the passive leak current, and I_{app} is the injected current (in $\mu A/cm^2$). A noise term $c\xi(t)$ of unspecified origin is included. The random variable $\xi(t)$ is uniformly distributed between -1, and $+1$ and is temporally uncorrelated. The noise amplitude is given by the parameter c, in simulations $c = 1$ to 1.5.

The symbol ΣI_{syn} represents the sum over all synaptic currents that each cell receives, hence is different in each of the four cells. The network connectivity is given by the "wiring diagram" of Fig. 5. Therefore, for RTC, $\Sigma I_{syn} = I_{STC\to RTC} + I_{ITC\to RTC} + I_{PC\to RTC}$; for STC, $\Sigma I_{syn} = I_{PC\to STC} + I_{RTC\to STC}$; for ITC, $\Sigma I_{syn} = I_{PC\to ITC} + I_{RTC\to ITC}$; and for PC, $\Sigma I_{syn} = I_{STC\to PC} + I_{ITC\to PC}$. We assume that RTC elicits the $GABA_A$-type inhibitory synaptic current, STC and ITC give rise to the fast AMPA-type excitatory synaptic current, while PC projects to RTC, STC and ITC via the slow NMDA-type excitatory synaptic current.

Table 1. Intrinsic Parameters (Conductances in mS/cm^2, Voltage in mV)

Fig.	Cell Type	g_L	V_L	g_{NaP}	g_{KS}	τ_m	Spike Curnt	σ	g_{Na}	g_K	g_T	g_A
6–7	RTC	0.1	−60	0.1	14	6	HH	0	72	30	0	0
	ITC	0.33	−70	0.3	14	16	T	0	200	250	0	0
	STC	0.1	−70	0	0	–	HH	3	42	20	0.4	0
	PC	0.1	−60	0	0	–	HH	3	42	20	0	0.3
8	RTC	0.1	−65	0.4	36	6	HH	3	120	26	0	0
	ITC	0.33	−70	0.5	34	10	T	0	200	250	0	0
	STC	0.1	−55	0.2	34	10	HH	3	120	26	0	0
	PC	0.1	−67	0	0	–	TWMM	3	120	26	0	0

Table 2. Synaptic parameters

Fig.	g_{STC} PC	g_{ITC} PC	g_{STC} RTC	g_{ITC} RTC	g_{PC} RTC	g_{PC} STC	g_{PC} ITC	g_{RTC} STC	g_{RTC} ITC
6	0.1	0.1	–	–	–	–	–	–	–
7	0.1	0.1	0.05	2	0	0	0	1.3	0.5
8	0.04	0.04	0.1	0.1	0.3	0.4	0.4	0.2	0.2

To complete the model description, the parameter values used in the simulations are listed in Table 1 and 2.

Acknowledgments: Supported by NIH-NINCDS NS13742 to R.L., U.R.; ONR N0014-90J-1194 to X.-J.W. and support from Commissariat a L'Energie Atomique D.S.V. to M.J.

References

Bienenstock E, Von der Malsburg C (1986) Statistical coding and short-term synaptic plasticity: a scheme for knowledge representation in the brain. In: Bienenstock E, Fogelman F, Weisbuch G (eds) Discordered systems and biological organization. pp 247–272. Les Houches: Springer-Verlag

Bressler SL, Freeman WJ (1980) Frequency analysis of olfactory system EEG in cat, rabbit and rat. Electroencephalogr Clin Neurophysiol 50:19–24

Cajal SR (1929) Etude sur la neurogénese de quelques vertébrés. Thomas, Springfield

Castaigne P, Buge A, Escourolle R, Masson M (1962) Ramollissement pédonuclaire médian, tegmento-thalamique avec ophtalmoplégie et hypersomnie. Rev Neurol 106:357–367

Connor JA, Walter D, McKown R (1977) Neural repetitive firing: modifications of the Hodgkin-Huxley axon suggested by experimental results from crustacean axons. Biophys J 18:81–102

Crick F, Koch C (1990) Some reflections on visual awareness. Cold Spring Harbor Symp Quant Biol 55:953–962

Deschênes M, Hu B (1990) Electrophysiology and pharmacology of the corticothalamic input to lateral thalamic nuclei: an intracellular study in the cat. Eur J Neurosi 2:140–152

Deschênes M, Madariage-Domich A, Steriade M (1985) Dendrodendritic synapses in the cat reticularis thalami nucleus: A structural basis for thalamic spindle synchronization. Brain Res 334:165–168

Eckhorn R, Bauer R, Jordan W, Brosch M, Kruse W, Munk M, Reitbock HJ (1988) Coherent oscillations: A mechanism of feature linking in the visual cortex? Biol Cybernet 60:121–130

Edelman GM (1987) Neuronal darwinism: The theory of neuronal group selection. Basic Books, New York

Facon E, Steriade M, Wertheim N (1958) Hypersomnie prolongée engendrée par des lésions bilatérales due systèm activateur médial le syndrome thrombotique de la biffurcation du tronc basilaire. Rev Neurol 98:117–133

Galambos R, Makeig S, Talmachoff PJ (1981) A 40-Hz auditory potential recorded from the human scalp. Proc Natl Acad Sci (USA) 78:2643–2647

Ghose GM, Freeman RD (1992) Oscillatory discharge in the visual system: Does it have a functional role? J Neurophysiol 68:1558–1574

Gray CM, Singer W (1989) Stimulus-specific neuronal oscillations in orientation columns of cat visual cortex. Proc Natl Acad Sci USA 86:1698:1702

Gray CM, Konig P, Engel AK, Singer W (1989) Oscillatory responses in cat visual cortex exhibit inter-columnar synchronization which reflects global stimulus properties. Nature 338:334–337

Harris WA (1987) Neurogenetics. In: Adelman G (ed) Encyclopedia of Neuroscience. Birkhäuser, Basel pp 791–793

Heilman KM, Balenstein E (1993) Clinical Neuropsychology, Oxford Univ. Press, New York, Oxford

Hodgkin AL, Huxley AF (1952) A quantitative description to conductance and excitation in nerve. J Physiol (London) 117:500–544

Krieg WJS (1966) Functional neuroanatomy. Brain Books, Pantagraph Printing, Bloomington, Illinois

Kristofferson AB (1984) Quantal and deterministic timing in human duration discrimination. Ann NY Acad Sci 423:3–15

Lande R (1979) Quantitative genetic analysis of multivariate evolution, applied to brain-body size allometry. Evolution 33:400–416

Llinás R (1987) "Mindness" as a functional state of the brain. In: Blakemore C, Greenfield SA (eds) Mindwaves. Basil Blackwell, Oxford pp 339–358

Llinás R (1990) Intrinsic electrical properties of mammalian neurons and CNS function. In: Fidia Research Foundation Neuroscience Award Lectures. Vol 4, Raven Press, New York pp 1–10

Llinás R, Paré D (1991) Of dreaming and wakefulness. Neuroscience 44:521–535

Llinás R, Ribary U (1992) Rostrocaudal scan in human brain: a global characteristic of the 40-Hz response during sensory input. In: Basar E, Bullock T (eds) Induced rhythms in the brain. Chapter 7, Birkhäuser: Boston pp 147–154

Llinás R, Ribary U (1993a) Perception as an oneiric-like state modulated by the senses. In: Large-scale neuronal theories of the brain. Boston, MIT Press, in press

Llinás R, Ribary U (1993b) Coherent 40-Hz oscillation characterizes dream state in humans. Proc Natl Acad Sci USA 90:2078–2081

Llinás R, Sugimori M (1980) Electrophysiological properties of *in vitro* Purkinje cell somata in mammalian cerebellar slices. J Physiol (London) 305:171–195

Llinás R, Grace AA, Yarom Y (1991) *In vitro* neurons in mammalian cortical layer 4 exhibit intrinsic activity in the 10 to 50 Hz frequency range. Proc Natl Acad Sci USA 88:897–901

Mountcastle VB, Hennemann E (1949) Pattern of tactile representation in thalamus of cat. J Neurophysiol 12:85–100

Mountcastle VB, Hennemann E (1952) The representation of tactile sensibility in the thalamus of the monkey. J Comp Neurol 97:409–440

Pantev C, Makeig S, Hoke M, Galambos R, Hampson S, Gallen C (1991) Human auditory evoked gamma-band magnetic fields. Proc Natl Acad Sci (USA) 88: 8996–9000

Pellionisz A, Llinás R (1982) Space-time representation in the brain. The cerebellum as a predictive space-time metric tensor. Neuroscience 7:2949–2970

Penfield W, Rasmussen T (1950) The cerebral cortex of man. MacMillan, New York

Pinault D, Deschênes M (1992) Voltage-dependent 40-Hz oscillations in rat reticular thalamic neurons *in vitro*. Neuroscience 51:245–258

Ribary U, Ioannides AA, Singh KD, Hasson R, Bolton JPR, Lado F, Mogilner A, Llinás R (1991) Magnetic Field Tomography (MFT) of coherent thalamo-cortical 40-Hz oscillations in humans. Proc Natl Acad Sci USA 88:11037–11041

Scharfman HE, Lu S-M, Guido W, Adams PR, Sherman SM (1990) N-Methyl-D-asparate receptors contribute to excitatory postsynaptic potentials of cat lateral geniculate neurons recorded in thalamic sclices. Proc Natl Acad Sci (USA) 87:4548–4552

Singer W (1993) Synchronization of cortical activity and its putative role in information processing and learning. Ann Rev Physiol 55:349–374

Steriade M (1991) In: Peters A, Jones EG (eds) Cerebral cortex. Chapter 9, Plenum, New York pp 279–357

Steriade M, Parent A, Hada J (1984) Thalamic projections of reticular nucleus thalami of cat: A study using retrograde transport of horseradish peroxidase and double fluorescent tracers. J Comp Neurol 229:531–547

Steriade M, Jones EG, Llinás R (1990) Thalamic oscillations and signalling. John Wiley & Sons, New York

Steriade M, CurróDossi R, Paré D, Oakson G (1991) Fast oscillations (20–40 Hz) in thalamocortical systems and their potentiation by mesopontine cholinergic nuclei in the cat. Proc Natl Acad Sci USA 88:4396–4400

Steriade M, CurróDossi R, Contreras F (1993) Electrophysiological properties of intralaminar thalamocortical cells discharging rhythmic (40 Hz) spike-bursts at 1000 Hz during waking and rapid eye movement sleep. Neuroscience 56:1–9

Traub R (1977) Repetitive firing of Renshaw spinal interneurons. Biol Cybern 27:71–76

Traub R, Wong RKS, Miles R, Michelson H (1991) A model of a CA3 hippocampal neuron incorporating voltage-clamp data on intrinsic conductances. J Neurophysiol 66:637–650

Von der Malsburg C (1981) The correlation theory of brain function. Internal report, Max-Planck Institute for Biophysical Chemistry. Goettingen RFA

Wang X-J (1993) Ionic basis for the intrinsic 40-Hz neuronal oscillations. NeuroReport 5:221–224

Wang X-J (1994) Multiple dynamic modes of thalamic relay neurons: rhythmic bursting and intermittent phase-locking. Neuroscience 59:21–31

Wang X-J, Rinzel J (1993) Spindle rhythmicity in the reticularis thalami nucleus: synchronization among mutually inhibitory neurons. Neuroscience 53:899–904

Wilson JR, Friedlander MJ, Sherman SM (1984) Ultrastructural morphology of identified X- and Y-cells in the cat's lateral geniculate nucleus. Proc Roy Soc B221: 411–436

Yen CT, Conley M, Hendry SHC, Jones EG (1985) The morphology of physiologically identified GABAergic neurons in the somatic sensory part of the thalamic reticular nucleus in the cat. J Neurosci 5:2254–2268